

Photocatalytic Degradation of Organic Dyes Using Nanocrystalline Mg-Co Ferrite

Jadhav SD* and Patil RS

Department of Chemistry, Yashwantrao Chavan College of Science, Karad Shivaji University, Kolhapur, India

Abstract

The semiconducting Mg-Co ferrite nanoparticles prepared via controlled co-precipitation method. The X-ray diffraction and Transmission Electron Microscopy (SAED patterns) techniques were employed to study phase, composition and the average particle size of the resulting material. The photocatalytic degradation of methyl orange and Congo red dye were performed under illumination of visible light (Philips 250 Watt) as source of photons. The behavior of this reaction was pseudo first order and the maximum photodecolorization efficiency was 85.16% for methyl orange and 95.40 for Congo red in 60 min. at 30°C.

Keywords: X-ray Diffraction • SEM • Transmission Electron Microscopy (TEM) • Photocatalysis

Introduction

Water contamination is mainly caused due to toxic effluents drain by number of chemical, agricultural and textile industries. It has been reported that about 25% dye stuffs discharged directly into the environment by textile factory. Generally waste water generated by textile industry contains considerable amount of non-fixed dyes, especially azo dyes and a huge amount of inorganic salts. Also contains several non-biodegradable substrates that can be harmful to the environment. Their toxicity, stability to natural decomposition and persistence in the environment has been the cause of much concern to the society and regulation authorities all around the world [1-3]. Environmental problems associated with toxic organic pollutants in water and air is current issues to be solved for the development of a healthy environment. Photocatalytic oxidation is one of the emerging technologies for the decomposition of organic dyes such as Reactive black 5, Acid orange, Aniline yellow, Orange B, Methyl yellow, Methyl red, Methylen blue, Congo red and Methyl orange etc. Azo dyes represent about one-half of the dyes used in the textile industry. Among azo dyes, Methyl Orange (MO) is highly water soluble, even at very low concentrations, which hinder the penetration of light and therefore cause adverse effects on photosynthesis. Congo Red (CR) was the first synthetic dye that could dye cotton directly [4]. It is contained in wastewater effluents from the textile, printing and dyeing, paper, and rubber and plastics industries. CR is used in medicine as a biological stain and as an indicator since it turns from red-brown in a basic medium to blue in an acidic one. These are the different ways organic pollutants (dyes) continuously get added into water sources. Incomplete decomposition of organic pollutants may leads to formation of more toxic byproducts than the parent

pollutants. Therefore, in order to overcome such problem looking for metal oxide photocatalyst with strong photodegradation capacity is inevitable. For instance, Jang et al [5, 6]. Respectively demonstrated that $ZnFe_2O_4$ and $CaFe_2O_4$ systems are useful for solar photocatalytic degradation of pollutants. Similarly, in case of homo [7,8]. Composite ferrite systems, $CaFe_2O_4:MgFe_2O_4$ and $ZnFe_2O_4:SrTiO_3$ have been shown to be efficient and useful for photocatalytic water splitting. It has been reported [9]. Investigated the effects of cation distribution in $CdFe_2O_4$ [10]. Studied the magnetic properties of cadmium ferrite prepared by coprecipitation [11]. Reported on structural and magnetic properties of $CdFe_2O_4$ ferrites [12]. Reported the magnetic resonance investigation of cadmium ferrite. Cai et al. developed $ZnFe_2O_4$ via a reduction-oxidation method which showed degradation of Orange II dye [13]. Sharma et al. MFe_2O_4 (M=Co, Ni, Cu, Zn) prepared by sol-gel method used for degradation of Methyl blue dye [14]. Reported $NiFe_2O_4$ visible light assisted photocatalytic degradation of Safranin-O dye and remazol brilliant yellow at pH 2.5 [15]. $ZnFe_2O_4$ for degradation of Methyl orange dye [16]. Studied $CoFe_2O_4$ prepared by sol-gel method for degradation of methylene blue [17]. The ferrites offer an advantage of displaying the desirable optical absorption for the low energy photons ($h\nu \sim 2$ eV), and of exhibiting the well suited electronic structure desirable for photocatalytic applications [18]. This contrasts with the very popular anatase TiO_2 reference material, whose band gap of 3.2 eV allows only the absorption of UV light, corresponding to wavelengths lower than 388 nm [19]. On the other hand especially photocatalyst are non-magnetic such as semiconductors (TiO_2 , ZnO and ZnS) their separation and recovery after treatment is difficult [20]. Consequently, the problem of insufficient recovery not only leads to loss of photo catalyst but also

*Address to Correspondence: Jadhav SD, Department of Chemistry, Yashwantrao Chavan College of Science, Karad Shivaji University, Kolhapur, India; E-mail: sdjchemsuk@gmail.com

Copyright: © 2022 Jadhav SD, et al. This is an open-access article distributed under the terms of the creative commons attribution license which permits unrestricted use, distribution and reproduction in any medium, provided the original author and source are credited.

Received: 11 February, 2022, Manuscript No. JEH-22-54247; **Editor assigned:** 14 February, 2022, Pre QC No. JEH-22-54247 (PQ); **Reviewed:** 01 March, 2022, QC No.

JEH-22-54247; **Revised:** 11 April, 2022, Manuscript No. JEH-22-54247 (R); **Published:** 26 April, 2022, DOI: 10.37421/2684-4923.22.06.168

the residual photo catalyst become additional environmental problem. Therefore, the effective and complete decolonization of organic pollutants containing wastewater is an important and challenging task. To make full use of solar energy, many attempts have been made to prepare the narrow band gap ferrite semiconducting material that utilizes the much larger visible region. Some of the recent reports can be important indicators with respect to the potential of visible light photocatalytic application of the spinel ferrites. Spinel ferrites which are mixed oxides of iron and a single or numerous metals are one such example of visible-light absorbing inorganic semiconductors studied for their photo catalytic activity due to their attractive photochemical properties such narrow optical, band gap (~2.0 eV), good photochemical stability [21]. Recovery of photocatalyst and their relative stability in acidic and basic conditions. Magnetic and optoelectronic properties [22]. They have strong photodegradation capacities; also improve the degradation rate of pollutants, ease the from the reaction mixture after being used and enhance consequently they are very useful for the complete removal of organic pollutants [23-25]. To the best of our knowledge, as per the literature there are few reports has been cited in the literature on the photocatalytic properties of divalent metal ion doped cobalt ferrite nanoparticles under solar light irradiation. Accordingly, in this paper we reported photocatalytic degradation of azo dye using magnesium doped cobalt ferrite nanoparticles.

Materials and Methods

Materials

Methyl orange and Congo red dye was supplied by Sigma Aldrich which a physico-chemical characteristic that is has illustrated in Figure 1 and Table 1.

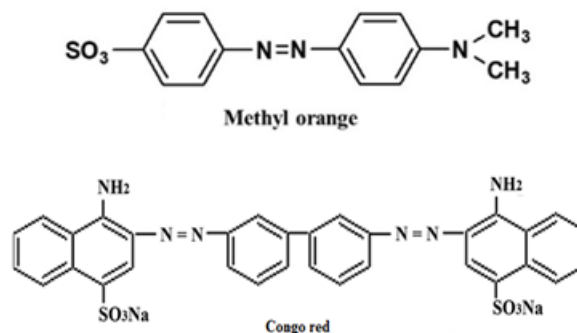


Figure 1. The structural formula of Methyl orange and Congo red dye.

Parameters	Methyl orange	Congo red
Synonym	547-58-0 Orange III	Direct red 28
Molecular Weight	327.33 g/mol	696.665 g/mol
Molecular formula	$C_{14}H_{14}N_3O_3Na$	$C_{22}H_{22}N_6Na_2O_6S_2$
Type	Acid dye	Acid-Basic Indicator
λ_{max}	460-470 nm	497-498 nm
Solubility in water	Soluble	Soluble

Table 1. Physico-chemical characteristics of the Methyl orange and Congo red dye.

Methods

The Mg-Co ferrite has been synthesized by using controlled co-precipitation technique [26]. The series of the photoreaction experiments were conducted by mixing 100 mL from aqueous solution of Methyl orange and Congo red with a suitable amount of $Mg_{0.5}Co_{0.5}Fe_2O_4$ nanopowder as suspension solution. In fact, the equilibrium time for this reaction was closely performed at 30 min as adsorption process. Visible light bulbs containing tungsten filament (Philips 250 W) were applied as a source of photons; it was connected at the top of the reactor chamber [27]. Light intensity value equal to 1.48×10^{-7} Ens. s^{-1} , which calculated by chemical actinometrical solution with regular intervals, certain amount of samples were collected and double separated by centrifuge to remove all photocatalyst from dye solutions [28]. The filtered dye solutions were analyzed to determine the residue concentration of dye by recording the absorbance at 464 nm and 500 nm using UV visible spectrophotometer. By depended on Langmuir-Henshelwood mechanism, the rate constant was determined [29].

And the Photo Decolorization Efficiency (PDE%) was calculated by the following equation (Figures 2 and 3) [30].

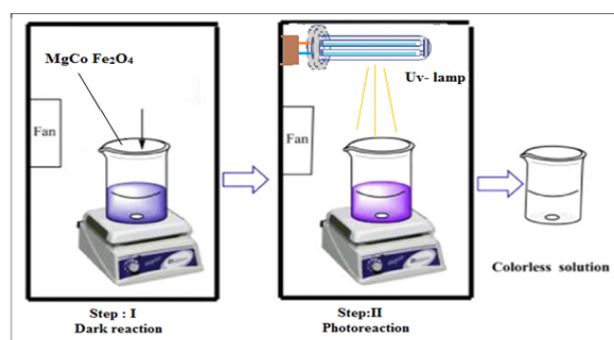


Figure 2. C_0 is an initial concentration of methyl Orange and Congo red dyes at no irradiation time (min). C_t is a concentration of the same dye at t time of irradiation.

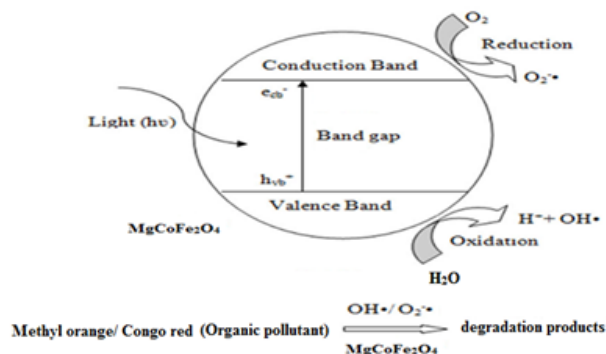


Figure 3. Solution of methyl orange and congo red with a suitable amount of $Mg_{0.5}Co_{0.5}Fe_2O_4$ nanopowder as suspension solution.

Results and Discussion

Characterization

The X-ray diffraction patterns of the system $Mg_{1-x}Co_xFe_2O_4$ ($x=0.0$ to 1.0) sintered at $600^\circ C$. All the indexed diffraction peaks corresponding to the (111), (220), (311), (400), (422) and (511) planes of polycrystalline spinel ferrite [31]. The X-ray lines found to be sharp which makes detection of phases easy. All spinel composition shows (311) peak is the more intense one. The d_{hkl} and 2θ values were compared with the values reported in the literature (cubic, $MgFe_2O_4$, JCPDS file No. 73-1720) and (cubic, $CoFe_2O_4$, JCPDS file No. 22-1086). The SEM micrograph shows the formation of polycrystalline grains. From this image, it can be seen that most of the grains are of size about ~ 30 nm Figure 4a. Transmission electron micrographs of $Mg_{0.5}Co_{0.5}Fe_2O_4$ system depict in Figure 4b and Figure 4c. The corresponding Selected Area Electron Diffractograms (SAEDs) are given as an inset. It is evident from these micrographs that all the synthesized samples have spherical particles ranging from 30 to 40 nm. The superimposition of the bright spot with Debye ring pattern indicates polycrystalline nature of the sample. Both the figures confirm that most of the particles are of size about 30 nm.

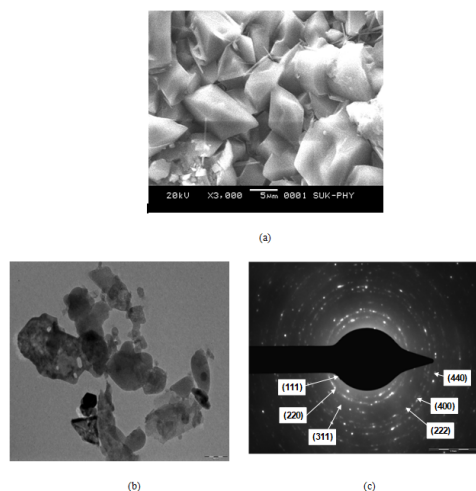


Figure 4. a) Scanning electron micrograph; b) Transmission electron micrograph; c) SAED pattern for $Mg_{0.5}Co_{0.5}Fe_2O_4$ sintered at $600^\circ C$.

Effect of irradiation time on photo degradation of Methyl orange and Congo red dyes

To test the Photo Catalytic (PC) properties of $Mg_{0.5}Co_{0.5}Fe_2O_4$, the kinetics of the degradation of a pollutant model, Methyl Orange (MO) and Congo Red (CR), were followed in water, under visible light (250 W) illumination. The intensity of the characteristic absorption bands of MO and CR centered at about 460-470 nm and 498-502 nm respectively [32]. Was measured every 30 min.

The degradation of MO solution was selected as reference and characteristic absorption of MO solution at about 464 nm was selected for monitoring adsorption and photocatalytic degradation process. A significant decrease in transmittance at about 460 nm can be assigned to absorption of light caused by the excitation of electrons from valence band to the conduction band of MO solution (Figure 4).

For CR there was complete absorption of light by CR solution, the absorption peak at 500 nm disappears and no peak shift can be detected after degradation treatment (Figure 5). A further comparison reveals that $\sim 80\%$, and $\sim 90\%$ degradation of methyl orange and Congo red within 120-150 min of irradiation respectively (Figure 6).

The increase of the pH value after visible light irradiation is due to the reduction of surface acidic groups in the ferrite powders, which were introduced during the preparation [33].

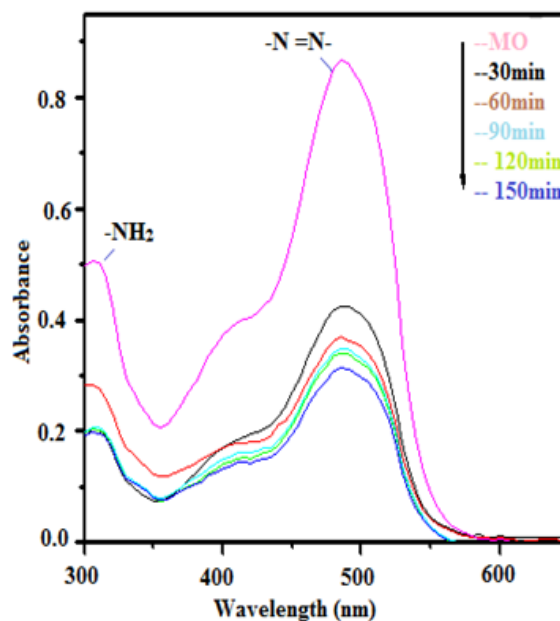


Figure 5. Effect of irradiation time on Methyl Orange dye.

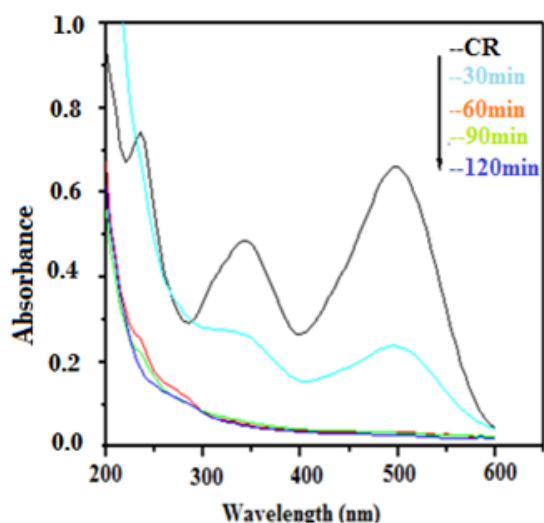


Figure 6. Effect of irradiation time on Congo red dye.

Effect of catalyst dose on the photo decolorization rate of methyl orange and congo red dyes

As seen in Figure 7 and Figure 8 the increased the doses of catalyst from range (0.5-2.5 g) in aqueous solution of methyl orange and Congo red dyes solution were raised the decolonization speed. This behavior indicates to find the many active sites of catalyst surface with increasing the dose. The transmitted light in dye solution is easy transmitted, hence, that entirely leads to enhance the producing of hydroxyl radical. This case will accelerate the decolorization of the dye according to the first possible of Langmuir-Hinshelwood (L-H) kinetics model [34]. The maximum rate constant and PDE% are found at dose 2.0 g/100 mL of $Mg_{0.5}Co_{0.5}Fe_2O_4$ and 85.16% at 70 min and 95.40% at 60 min. From the other hand, after using 2.5 mg/100 mL of catalyst powder, the rate of reaction depresses, that based on the raised of the solution turbidity and declined the transmittance of light, which cause inhibited the hydroxyl radical formation and this effect is called screen effect [35-37].

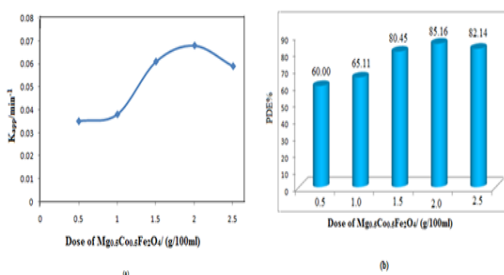


Figure 7. Effect of catalyst dose on the a) apparent rate constant of reaction; b) PDE%, at conditions: cat. dose=(0.5-2.5) g/100 mL, methyl orange dye conc.=30 ppm, initial pH of solution=5.5 and T=303 K.

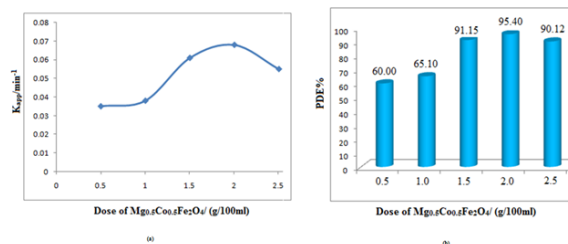


Figure 8. Effect of catalyst dose on the (a) apparent rate constant of reaction (b) PDE%, at conditions: cat. Dose =(0.5-2.5) g/100 mL, Congo red dye conc=30 ppm, initial pH of solution=5.5 and T=303K.

Reusability study of catalyst

The effect of catalyst used after number of runs on the dye solution at conditions: dose (2.0) g/100 mL, conc=30 ppm, initial pH of solution=5.5 and T=303 K. The PDE% for Methyl orange is 85.16% and PDE% of Congo red 95.40%. Photodegradation rate further goes on decreases after each successive run (Figures 9 and 10).

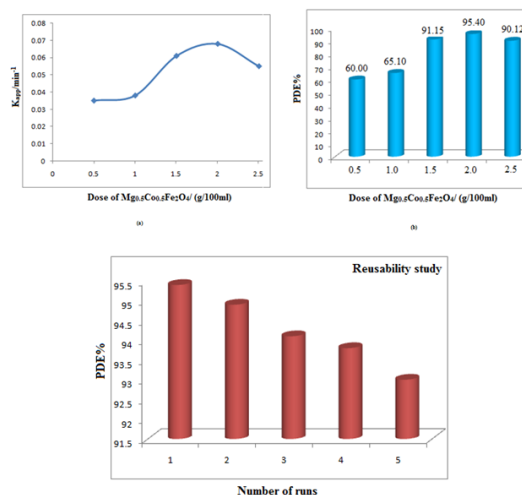


Figure 9. Effect reuse of catalyst at conditions: dose (2.0) g/100 mL, conc=30 ppm, initial pH of solution=5.5 and T=303 K for Methyl orange dye.

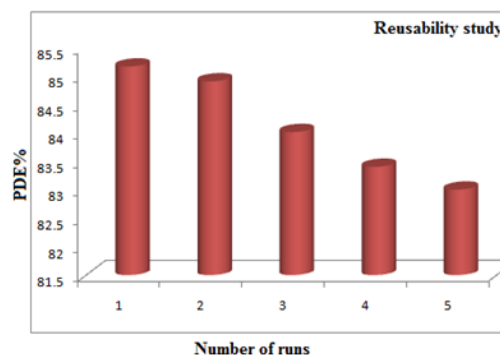


Figure 10. Effect reuse of catalyst at conditions: dose (2.0) g/100 mL, conc. = 30 ppm, initial pH of solution=5.5 and T=303 K for Congo red dye.

Mechanism

In order to form hydroxyl radical on $Mg_{0.5}Co_{0.5}Fe_2O_4$, Figure 11 nanopowder surface must focus a light on the suspension solution. On the basis of the photodecolorization processes described in reference, various redox process can be conducted on surface of photoconductor under illumination of visible light. Firstly, electron-hole pair (exciton) on catalyst surface was generated. The electron-hole pair is separated by reacting with the other species (H_2O , O_2) in series steps then formed groups of radical intermediates like: superoxide ion O_2^- hydrogen peroxide radical (hydroperoxy radical) then leads hydroxyl radical which has a more activity than HO_2 [38,39].

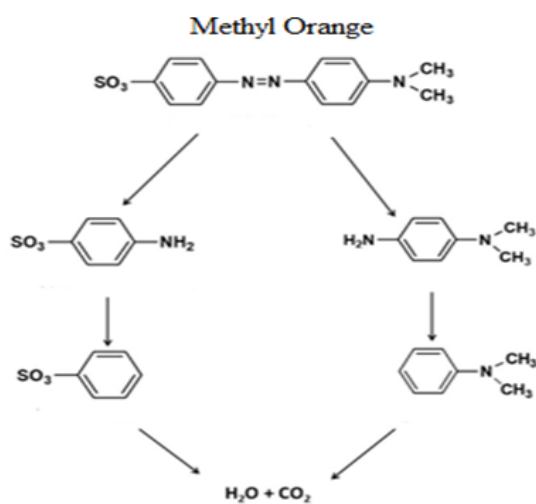


Figure 11. Methyl orange.

Conclusion

In this study, the main conclusions were observed that the photocatalytic decolorization process of methyl orange and Congo red dyes in suspension solution of $Mg_{0.5}Co_{0.5}Fe_2O_4$ nanopowder under visible light system were carried out. This photoreaction is found to be endothermic and obeyed the pseudo first order with low activation energy. In case of methyl orange the rate of reaction is moderate and same for Congo red it is fast. The PDE% for Methyl orange is 85.16% \tilde{A} than PDE% of Congo red 95.40%. Further reuse of catalyst the rate of photodegradation goes on decreases after each successive run. The suitable mechanism was suggested to obtain the depolarization and degradation of this dye with form CO_2 and H_2O (mineralization process) at final pH equal to 7.4.

Acknowledgement

Author (SDJ) thankful to the department of chemistry, Yashwantrao Chavan College of Science, Karad.

References

- Shandilya, Pooja, Sambyal Shabnam, Sharma Rohit, and Kumar Amit, et al. "Recent Advancement on Ferrite Based Heterojunction

- for Photocatalytic Degradation of Organic Pollutants: A Review." *Ferrite: Nanostructures Tunable Properties Diverse Appl* 112 (2021): 121-161.
- Gupta, Shipra Mital, and Tripathi Manoj. "A Review of TiO_2 Nanoparticles." *Chinese Sci Bulletin* 56 (2011): 1639-1657.
- Pham, Thanh-Dong, Van Noi Nguyen, Kumar Sharma Ajit, and Dao Van-Duong. "Advanced nanomaterials for green growth." *J Chem* (2020).
- Borse, PH, Lim KT, Yoon JH, and Bae JS, et al. "Investigation of the Physico-Chemical Properties of $Sr_2FeNb_{1-x}W_xO_6$ ($0.0 \leq x \leq 0.1$) for Visible-Light Photocatalytic Water-Splitting Applications." *J Korean Physical Society* 64 (2014): 295-300.
- Jang, Jum-Suk, H Borse Pramod, Lee Jae-Sung, and Jung Ok-Sang, et al. "Synthesis of nanocrystalline $ZnFe_2O_4$ by Polymerized Complex Method for its Visible Light Photocatalytic Application: An Efficient Photo-Oxidant." *Bulletin Korean Chem Society* 30 (2009): 1738-1742.
- Kim, Hyun Gyu, H Borse Pramod, Suk Jang Jum, and Duck Jeong Euh et al. "Fabrication of $CaFe_2O_4/MgFe_2O_4$ bulk heterojunction for enhanced visible light photocatalysis." *Chem Commun* 39 (2009): 5889-5891.
- Boumaza, S, Boudjemaa A, Bouguelia A, and Bouarab R, et al. "Visible light induced hydrogen evolution on new hetero-system $ZnFe_2O_4/SrTiO_3$." *Appl Energy* 87 (2010): 2230-2236.
- Cheng, Ching, and Liu Ching-Sheng. "Effects of cation distribution in $ZnFe_2O_4$ and $CdFe_2O_4$: ab initio studies." *J Physics: Conf Series* 145 (2009) 012028.
- Yokoyama, M, Sato Tetsuya, Ohta E, and Sato T. "Magnetization of Cadmium Ferrite Prepared by Coprecipitation" *J Appl Phys* 80 (1996): 1015-1019.
- Gadkari, Ashok, Shinde Tukaram, and Vasambekar Pramod. "Influence of rare-earth ions on Structural and Magnetic Properties of $CdFe_2O_4$ Ferrites." *Rare Metals* 29, (2010): 168-173.
- Silva, O, Lima ECD, and Morais PC. "Cadmium ferrite ionic magnetic fluid: Magnetic resonance investigation" *J Appl Phys* 93 (2003): 8456-8458.
- Cai, Chun, Zhang Zhuoyue, Liu Jin, and Shan Ni, et al. "Visible light-assisted Heterogeneous Fenton with $ZnFe_2O_4$ for the Degradation of Orange II in Water." *Appl Catalysis B: Environ* 182 (2016): 456-468.
- Sharma, Rimi, Bansal S, and Singhal Sonal. "Tailoring the Photo-Fenton Activity of Spinel Ferrites (MFe_2O_4) by Incorporating Different Cations (M= Cu, Zn, Ni and Co) in the structure." *Rsc Adv* 5 (2015): 6006-6018.
- Dhiman, Manisha, Goyal Ankita, Kumar Vinod, and Singhal Sonal. "Designing Different Morphologies of $NiFe_2O_4$ for Tuning of Structural, Optical and Magnetic Properties for Catalytic Advancements." *J Chem* 40 (2016): 10418-10431.
- Jadhav, SD, Hankare PP, Patil RP, and Sasikala R. "Effect of Sintering on Photocatalytic Degradation of Methyl Orange Using Zinc Ferrite." *Materials lett* 65 (2011): 371-373.
- Garcia-Muñoz, Patricia, Fresno Fernando, A Peña O'Shea Víctor, and Keller Nicolas. "Ferrite Materials for Photoassisted Environmental and Solar Fuels Applications." *Top Curr Chem* (2020): 107-162.
- Harish, KN, Bhojya Naik HS, Prashanth Kumar PN, and Vishwanath R, et al. "Optical and photocatalytic properties of $CdFe_2O_4$ nanocatalysts: potential application in water treatment under solar light irradiation." *Arch Appl Sci Res* 5 (2013): 42-51.
- Patil, RP, Pandav RS, Jadhav AV, and Jadhav SD, et al. "Investigation of Structural, Magnetic and Photocatalytic Properties of Al Substituted Cobalt Ferrites." *Materials Focus* 5, (2016): 11-16.
- Mamba, G, and Mishra AK. "Graphitic Carbon Nitride ($G-C_3N_4$) Nanocomposites: A New and Exciting Generation of Visible Light Driven Photocatalysts for Environmental Pollution Remediation." *Appl Catalysis B: Environ* 198 (2016): 347-377.

20. Ombaka, Lucy M, Dillert Ralf, Robben Lars, and W Bahnemann Detlef. "Evaluating Carbon Dots as Electron Mediators in Photochemical and Photocatalytic Processes of NiFe₂O₄." *Appl Materials* 8 (2020): 031105.
21. Ismael, M. "Solar Energy Materials and Solar Cells Ferrites as Solar Photocatalytic Materials and their Activities in Solar Energy Conversion and Environmental Protection: A Review." *Sol Energy Mater Sol Cells* 219 (2021): 110786.
22. Kefeni, Kebede Keterew, and B Mamba Bhokie. "Photocatalytic Application of Spinel Ferrite Nanoparticles and Nanocomposites in Wastewater Treatment." *Sustain Materials Technol* 23 (2020): e00140.
23. Kubacka, Anna, Fernandez-Garcia Marcos, and Colon Gerardo. "Advanced Nanoarchitectures for Solar Photocatalytic Applications." *Chem Rev* 112 (2012): 1555-1614.
24. Hankare, PP, PD Kamble, MR Kadam, KS Rane, and PN, Vasambekar. "Effect of sintering temperature on the properties of Cu-Co ferrites prepared by oxalate precipitation method." *Material Lett* 61 (2007): 2769-2771.
25. Abbas, Naseem, Rubab Nida, Sadiq Natasha, and Manzoor Suryyia, et al. "Aluminum-Doped Cobalt Ferrite as an Efficient Photocatalyst for the Abatement of Methylene Blue." *Water* 12 (2020): 2285.
26. Martinson, Kirill D, D Beliaeva Anna, D Sakhno Daria, and D Beliaeva Irina, et al. "Synthesis, Structure, and Antimicrobial Performance of Ni_xZn_{1-x}Fe₂O₄ (x= 0, 0.3, 0.7, 1.0) Magnetic Powders toward *E. coli*, *B. cereus*, *S. citreus*, and *C. tropicalis*." *Water* 14 (2022): 454.
27. Ahmed, Samina. "Photo Electrochemical Study of Ferrioxalate Actinometry at A Glassy Carbon Electrode." *J Photochem Photobiol A: Chem* 161 (2004): 151-154.
28. Mahammed, Bedour A, and M Ahmed Luma. "Enhanced Photocatalytic Properties of Pure and Cr-Modified Zns Powders Synthesized by Precipitation Method." *J Geosci Environ Protect* 5 (2017): 101.
29. Li, Jinmei, Lei Tao, Wang Jiaou, and Wu Rui, et al. "In-plane crystal field constrained electronic structure of stanene." *Appl Phy Lett* 116 (2020): 101601.
30. Alemi, Abdolali, Woo Joo Sang, Khademinia Shahin, and Dolatyari Mahboubeh, et al. "Sol-Gel Synthesis, Characterization, and Optical Properties of Gd³⁺-doped CdO Sub-Micron Materials." *Int Nano Lett* 3 (2013): 1-6.
31. Ahmed, Luma Majeed. "Photo-decolourization kinetics of acid red 87 dye in ZnO suspension under different types of UV-A light." *Asian J Chem* 30 (2018): 2134-2140.
32. Jasim, Khlowd Mohammed, and Luma M. Ahmed. "TiO₂ nanoparticles sensitized by safranin O dye using UV-A light system." *IOP Conf Ser: Mater Sci Eng* 571 (2019): 012064.
33. Jawad, TM, and LM Ahmed. "Synthesis of WO₃/TiO₂ nanocomposites for Use as Photocatalysts for Eosin Yellow Dye Degradation." *IOP Conf Ser: Mater Sci Eng*, 1067, (2021): 012153.
34. Jasim, Khlowd Mohammed, and M Ahmed Luma. "TiO₂ Nanoparticles Sensitized by Safranin O Dye Using UV-A Light System." *IOP Conf Ser: Mater Sci Eng* 571 (2019): 012064.
35. Radović, Miljana D, Jelena Z Mitrović, Kostić Miloš M, and V Bojić Danijela, et al. "Comparison of ultraviolet radiation/hydrogen peroxide, Fenton and photo-Fenton processes for the decolorization of reactive dyes." *Hemijiska industrija* 69 (2015): 657-665.
36. Khlowd Mohammed Jasim and M Ahmed Luma. "TiO₂ nanoparticles sensitized by safranin O dye using UV-A light system." In *IOP Conf Ser: Mater Sci Eng* 571 (2019): 012064.
37. Dojcinovic, Milena P, Z Vasiljevic Zorka, P Pavlovic Vera, and Barisic Dario, et al. "Mixed Mg-Co spinel ferrites: structure, morphology, magnetic and photocatalytic properties." *J Alloys Compounds* 855 (2021): 157429.
38. Harraz, FA, Mohamed RM, Rashad MM, and Wang YC, et al. "Magnetic nanocomposite based on titania-silica/cobalt ferrite for photocatalytic degradation of methylene blue dye." *Ceramics Int* 40 (2014): 375-384.
39. Swathi, S, Yuvakkumar R, Senthil Kumar P, and Ravi G, et al. "Annealing temperature effect on cobalt ferrite nanoparticles for photocatalytic degradation." *Chemosphere* 281 (2021): 130903.

How to cite this article: SD,Jadhav, RS Patil. "Photocatalytic Degradation of Organic Dyes Using Nanocrystalline Mg-Co Ferrite ." *J Environ Hazard* 6 (2022) : 168